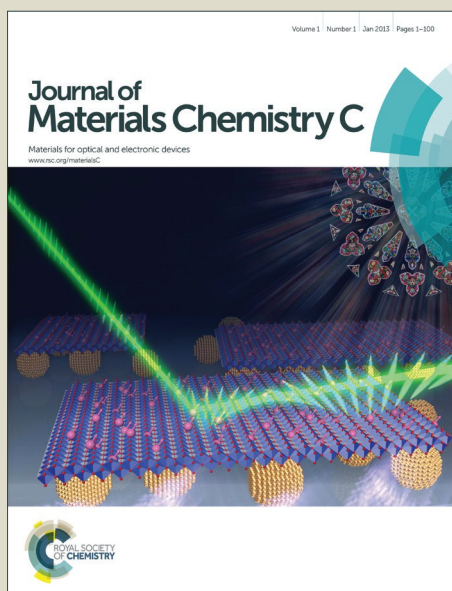


Journal of Materials Chemistry C

Accepted Manuscript



This article can be cited before page numbers have been issued, to do this please use: R. Kumar, S. Sandhu, P. Singh and S. Kumar, *J. Mater. Chem. C*, 2016, DOI: 10.1039/C6TC01891B.



This is an *Accepted Manuscript*, which has been through the Royal Society of Chemistry peer review process and has been accepted for publication.

Accepted Manuscripts are published online shortly after acceptance, before technical editing, formatting and proof reading. Using this free service, authors can make their results available to the community, in citable form, before we publish the edited article. We will replace this *Accepted Manuscript* with the edited and formatted *Advance Article* as soon as it is available.

You can find more information about *Accepted Manuscripts* in the [Information for Authors](#).

Please note that technical editing may introduce minor changes to the text and/or graphics, which may alter content. The journal's standard [Terms & Conditions](#) and the [Ethical guidelines](#) still apply. In no event shall the Royal Society of Chemistry be held responsible for any errors or omissions in this *Accepted Manuscript* or any consequences arising from the use of any information it contains.



Journal Name

ARTICLE

Water dispersed fluorescent organic aggregates for detection of picomolar ClO_4^- in water, soil and blood serum and atto g by contact mode

Rahul Kumar, Sana Sandhu, Prabhpreet Singh* and Subodh Kumar*

Received 00th January 20xx,
Accepted 00th January 20xx

DOI: 10.1039/x0xx00000x

www.rsc.org/

Fluorescent organic aggregates (FOAs) of **CS-1** have been used for the fluorescence based selective estimation of ClO_4^- ions. **CS-1** undergoes self-aggregation to form FOAs ($\phi = 0.35$) with diameter 140 ± 50 nm in aqueous medium. Dynamic light scattering and field emission scanning electron microscopic studies reveal that FOAs of **CS-1** undergo further aggregation to form larger particles on addition of ClO_4^- (10 pM – 1 nM concentration) but at higher concentrations of ClO_4^- ions, these FOAs undergo dis-aggregation to give finally molecularly dissolved complex of **CS-1** and ClO_4^- . This ClO_4^- induced aggregation – dis-aggregation process of FOAs of **CS-1** is associated with super-amplified fluorescence quenching following two domains of non-linear complexation with K_{sv} values $2.42 \times 10^8 \text{ M}^{-1}$ and $3.59 \times 10^5 \text{ M}^{-1}$ and variation in Life time measurements of FOAs of **CS-1** at different concentrations of ClO_4^- . The lowest limit of detection is 10 pM in solution and $6 \times 10^{-18} \text{ g/cm}^2$ by contact mode method with selectivity of ~ 10000 over other inorganic anions and allows quantitative measurement of ClO_4^- ions using front surface steady state fluorescence of paper strips coated with **CS-1**. FOAs of **CS-1** find applications in determination of ClO_4^- from tap water, soil and also in the presence of blood serum. Probe **CS-2**, which differs from **CS-1** in lack of three methyl groups on the m-phenylene spacer, shows poor sensitivity (LOD 1.6 μM) towards ClO_4^- . DFT studies of **CS-1** and **CS-2** and their complexes with ClO_4^- reveal the effect of methyl substituents on their geometries.

Introduction

The development of fluorescent probes based on single molecular interaction with a stimulant has attracted considerable research interest over the past few decades¹⁻¹⁷. Due to strong interactions of anions with water molecules, the design of anion recognition probes active in water with high sensitivity and selectivity towards an anion is still a challenge. Compared with these optical probes which remain dissolved at molecular level, the fluorescent organic aggregates (FOAs) which remain dispersed in water have received increasing attention¹⁸⁻²⁵ owing to their higher selectivity and sensitivity through combination of stimulant induced changes in their aggregate state and molecular interactions and thus result in change in their optical properties at significantly lower concentrations of the stimulant.

Fluorescent organic aggregates (FOAs) can be generated through molecular self-assembly via a range of interactions, such as electrostatic interactions, hydrogen bonding,

hydrophobic interactions, and covalent coupling etc. Even, the mixing of a charged organic nano particles with oppositely charged stimulant can induce aggregation – disaggregation process^{26,27} resulting in aggregation / disaggregation induced emission enhancement or quenching. Also, the interaction of a FOA with single stimulant molecule can result in exciton transfer²⁸⁻³¹ to large number of probe molecules in FOA resulting in amplification of the signal.

Amongst anions, ClO_4^- disrupts thyroid iodine uptake in human beings due to its ability to substitute iodide ion and has increased concerns to its effects on human health^{32,33}. However, due to its weak coordination behavior, the efforts to design molecules for its qualitative encapsulation³⁴⁻³⁷ and quantitative detection have met with a limited success³⁸⁻⁴³. In none of these cases ClO_4^- ions could be determined below nano molar concentration and could be used for detection of ClO_4^- ions in the presence of blood serum. Recently, our group has shown that N-aryl benzimidazolium moieties linked through an appropriate spacer can be used for fluorescence based selective detection of ClO_4^- ions from tap water, fireworks, live cell imaging etc.^{39,40} Amongst other reports, Gao et al have also reported an imidazolium based chemosensor which undergoes ClO_4^- ions mediated aggregation induced fluorescence enhancement⁴². However, in none of these cases the detection limit for ClO_4^- ions could be attained in pico to nano molar concentration range and also probably due to strong interactions of the probe with blood serum, these could

*Department of Chemistry, UGC centre for advanced studies, Guru Nanak Dev University, Amritsar 143005, Punjab, India
Fax: (+91)91-183-228880
E-mail: subodh_gndu@yahoo.co.in.

† Footnotes relating to the title and/or authors should appear here.
Electronic Supplementary Information (ESI) available: [the spectra of **CS-1**, **CS-2** and photophysical studies]. See DOI: 10.1039/x0xx00000x

ARTICLE

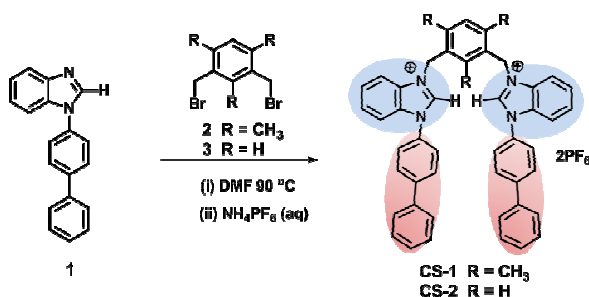
not be used for detection of ClO_4^- ions in the presence of blood serum.

Herein, we report new chemosensors **CS-1** and **CS-2**, which differ only in substituents on the spacer between two benzimidazolium moieties but **CS-1** owing to its unique ClO_4^- induced aggregation - disaggregation behaviour in water [HEPES buffer (2% DMSO)] exhibits highly selective and sensitive fluorescence quenching. Conspicuously, chemosensor **CS-2**, like earlier reported chemosensors⁴⁰, does not form aggregates and shows poor sensitivity (poorer by $> 10^4$ times) towards ClO_4^- ions and highlights the significance of methyl groups present on the *m*-phenylene spacer in **CS-1** in achieving high sensitivity and selectivity.

CS-1 in water undergoes aggregation to form FOAs with a mixture of spherical and rod-like morphology (80-170 nm). DLS and FE-SEM studies reveal that aggregation of these FOAs is further enhanced in the presence of 10 pM to 1 nM perchlorate ions, as evident by increase in their size to $200 - 500 \pm 50$ nm. Subsequently, at higher concentrations of ClO_4^- ions (5 μM), these FOAs undergo dis-aggregation to form molecularly dissolved 1:1 complex of **CS-1** and ClO_4^- . This process of ClO_4^- ions induced aggregation - disaggregation (Scheme 1) is associated with continuous decrease in fluorescence of the solution of **CS-1** and allows determination of 10 pM concentration of ClO_4^- ions in solution phase and 6×10^{-18} g/cm² by contact mode method using paper strips coated with **CS-1** and quantitatively measuring front surface steady state fluorescence. Significantly, other anions viz. F^- , Cl^- , Br^- , I^- , CN^- , OH^- , H_2PO_4^- , NO_3^- , AcO^- , HSO_4^- , SO_4^{2-} , SCN^- etc show insignificant change in the fluorescence of **CS-1** and do not interfere in the estimation of ClO_4^- . **CS-1** could be used for estimation of ClO_4^- in drinking water, soil samples and in the presence of blood serum.

2. Results and Discussion

CS-1 was synthesized in 94% yield by heating a 2:1 mixture of compounds **1** and **2** in DMF at 90 °C under N_2 with subsequent anion exchange with PF_6^- (Scheme 2). The presence of NCH_2 singlet at δ 5.84 and benzimidazolium $\text{C}_2\text{-H}$ protons at δ 9.46 in its ^1H NMR spectrum and appearance of parent ion peak at 831.3148 in its HRMS spectrum confirm the formation of **CS-1**. Similar reaction of **1** with dibromide **3** gave chemosensor **CS-2**. The structures of chemosensors **CS-1** and **CS-2** have been confirmed by ^1H NMR, ^{13}C NMR, and HRMS



Scheme 2: Synthesis of chemosensors **CS-1** and **CS-2**

spectral data (Fig. S1-4, ESI[†]).

Before examining anion interaction studies of **CS-1** and **CS-2**, the optical properties of **CS-1** and **CS-2** were recorded in DMSO and binary mixtures of DMSO : H_2O (v/v) to rationalize the effect of aqueous medium. We have observed that with the increase in volume fraction of water from 0% to 98% in DMSO, the absorption intensity of **CS-1** continuously decreases and for the solutions containing $> 60\%$ water, the absorption spectrum becomes broadened (Fig. S5A, ESI[†]). In case of fluorescence spectra, we observed that as the volume fraction of water increased from 0-40%, the emission intensity of **CS-1** also increases with concomitant red-shift of the emission maxima by 10 nm from 430 nm to 440 nm. This could be assigned to the change in environment around the molecularly dissolved **CS-1** molecules (Fig. 1).

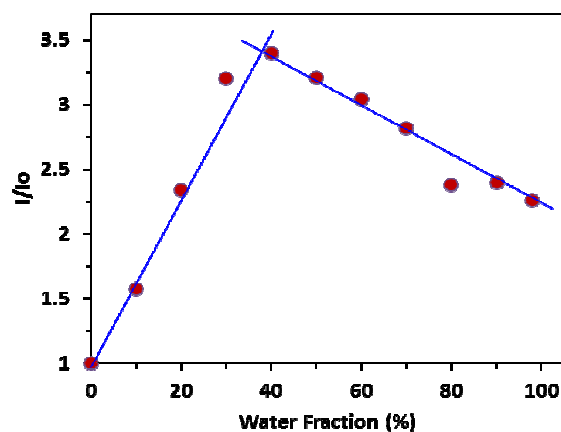
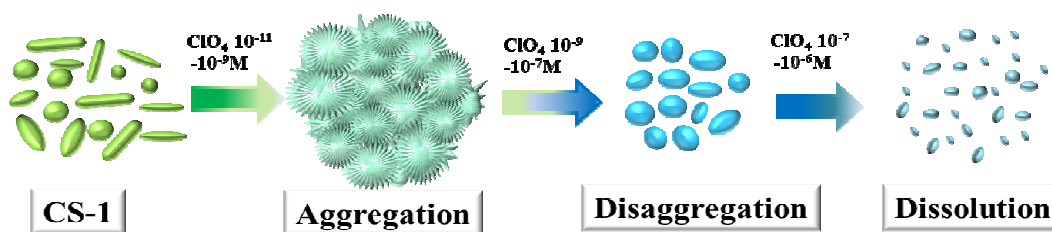


Fig. 1. Change in fluorescence intensity of **CS-1** with increasing volume fractions of water.



Scheme 1: Schematic presentation of mechanism of ClO_4^- interaction with **CS-1**

Journal Name

ARTICLE

Interestingly, further increase in water fraction from 40 to 98% in DMSO, the emission intensity decreases to a small extent along with red-shift of the emission maxima to 460 nm (Fig. SI 5B). These results indicate aggregation of **CS-1** to form fluorescent organic aggregates (FOAs) in aqueous media^{18–25}. In case of **CS-2** on increasing volume fraction of water to 50%, the emission maxima underwent gradual red-shift from 438 nm to 450 nm due to change in the environment around molecules and further increase in volume fractions of water did not affect the emission maxima or fluorescence intensity and points to non-aggregation of **CS-2** in water. Therefore, in case of **CS-1**, the increased hydrophobicity due to the presence

of three methyl substituents on the *m*-phenylene spacer directs its aggregation in water.

The aggregation of **CS-1** to form FOAs in water and their interaction with different concentrations of ClO_4^- ions have been confirmed by DLS experiments which have been truly supported by FE-SEM studies of the thin films prepared from these solutions and fluorescence techniques (solution phase and solid state). From DLS experiments we have observed that the solution of **CS-1** in water (2% DMSO) shows the formation of FOAs with size 140 ± 50 nm (Fig. 2C). FE-SEM images of the thin films of **CS-1** also reveal the formation of FOAs (a mixture of spherical and rod-like) with diameter 160 ± 50 nm (Fig. 2A–B).

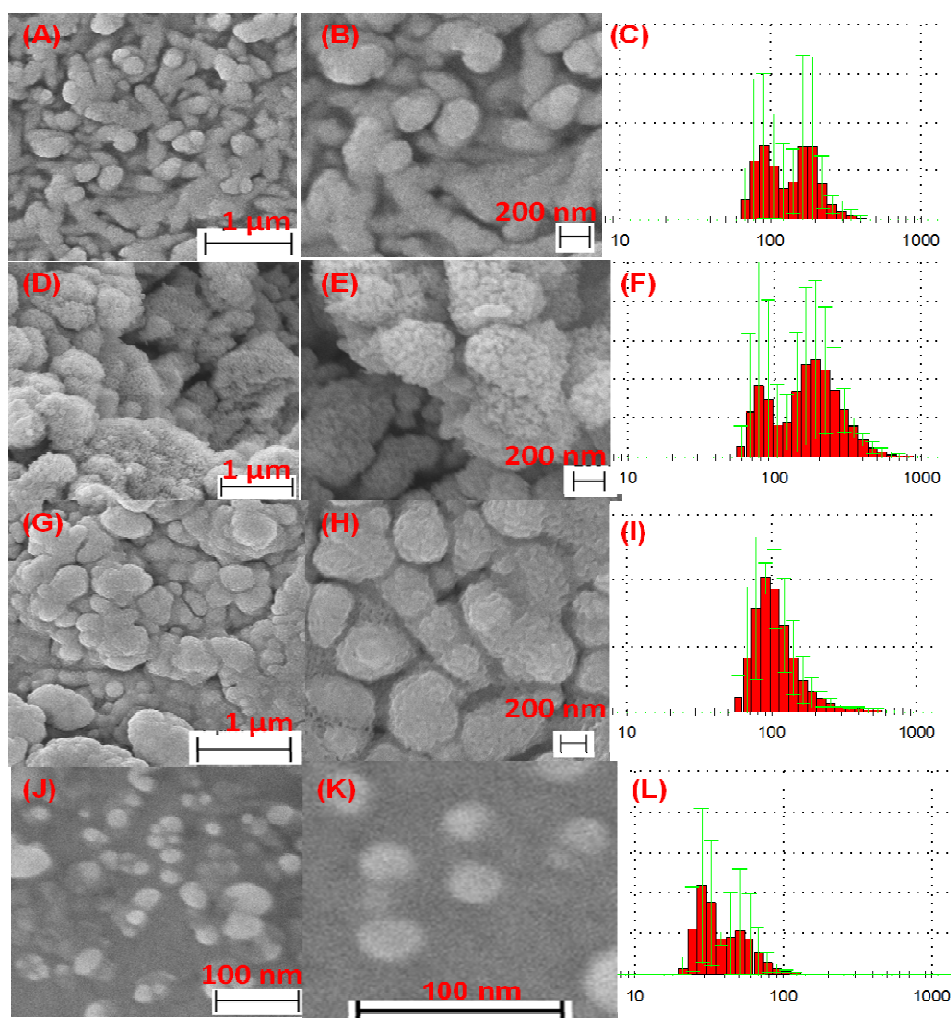


Fig 2. (A–C) SEM image and DLS graph of **CS-1** (5 μM); (D–F) SEM image and DLS graph of **CS-1** in the presence of ClO_4^- (5×10^{-11} M); (G–I) SEM image and DLS graph of **CS-1** in the presence of ClO_4^- (10^{-6} M); (J–L) SEM image and DLS graph **CS-1** in the presence of ClO_4^- (1×10^{-5} M).

Journal Name

ARTICLE

In FE-SEM the increasing concentration of **CS-1** in the solution during drying of the films may be responsible for small increase in size of the FOAs as compared to those observed in case of DLS experiments.

Interestingly, FE-SEM of FOAs of thin film of the solution of **CS-1** containing 5×10^{-11} M ClO_4^- shows the aggregation of FOAs to larger size particles (280 – 500 nm) and these are in consonance with DLS experiments pointing the formation of $200 - 500 \pm 50$ nm size aggregates (Fig. 2D-F). However, as we further increased the concentration of ClO_4^- ions to 1×10^{-6} M in the solution of **CS-1** (5 μM), the size of the FOAs decreased to 150 ± 40 nm, in consonance with 120 ± 40 nm size of FOAs as observed from DLS experiments (Fig. 2G-I). On further increasing the concentration of ClO_4^- ions to 10^{-5} M, the particles were well dispersed and their size was reduced to 30 – 60 nm as observed under both FE-SEM images and DLS experiments (Fig. 2J-L). Thus, **CS-1** in 98% aqueous medium undergo self-assembly to form FOAs which on addition of ClO_4^-

(5×10^{-11} M) undergo further aggregation and between 10^{-9} to 10^{-5} M ClO_4^- undergo disaggregation to molecularly dissolved state. Conspicuously, DLS results in HEPES buffer, reveal that the aggregates of only **CS-1** has size 165 ± 40 nm and on addition of 5×10^{-11} M ClO_4^- the size of aggregates is increased to 250–800 nm and in presence of 10^{-6} M ClO_4^- , the size of aggregates is reduced to 200 ± 100 nm and finally at 10^{-5} M ClO_4^- size of aggregates is further reduced to 60 ± 30 nm. Also, the average size of the aggregates of **CS-1** and **CS-1** + 10^{-5} M ClO_4^- ions remained stable even on recording DLS after 24h. (Fig. S6 ESI[†]).

The UV-Vis spectrum of FOAs of **CS-1** (2 μM) in HEPES buffer (0.05 M pH 7.4, 2% DMSO) showed an absorption maxima at 270 nm typical of aromatic moieties. The titration of solution of **CS-1** (2 μM) with NaClO_4 showed gradual decrease in absorbance at 270 nm associated with increase in absorbance between 320–650 nm with an isosbestic point at 290 nm (Fig. 3A). The plot of $\log[\text{ClO}_4^-]$ concentration vs A_0/A

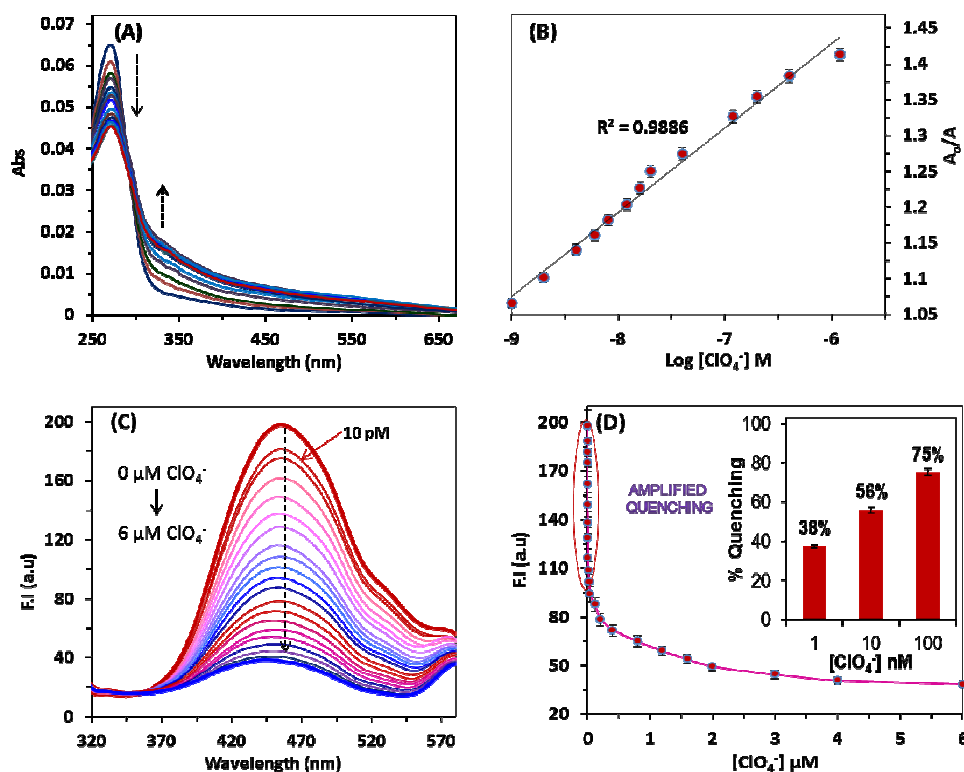


Fig 3. (A) Effect of gradual addition of ClO_4^- ions on the absorption spectrum of **CS-1** (2 μM HEPES buffer – 2% DMSO, pH 7.4); (B) plot of A_0/A vs $\log [\text{ClO}_4^-]$; (C) Effect of gradual addition of ClO_4^- ions on the emission spectrum ($\lambda_{\text{ex}} = 290$ nm) of **CS-1** (2 μM , HEPES buffer – 2% DMSO, pH 7.4); (D) plot of FI at 460 nm vs $[\text{ClO}_4^-]$ and inset shows decrease in FI of **CS-1** at 1, 10 and 100 nM concentration (error bars show $\sim 2.6\%$ error).

Journal Name

ARTICLE

Table 1 Comparison of LOD of ClO_4^- by **CS-1** with literature reports

S. No.	Journal Name	Phenomena	Solution (Detection limit)	Contact mode (detection limit)
1	Present work	Aggregation-disaggregation	10 pM (0.01 nM)	$6 \times 10^{-18} \text{ g cm}^{-2}$
2	Chem. Commun., 2014, 50, 5623-5625	aggregation	NR	No
3	Chem. Commun., 2014, 50, 13994-13997	Dis-aggregation	60 nM	$8 \times 10^{-10} \text{ g cm}^{-2}$
4	RSC Adv., 2013, 3, 14044-14047	Cavity based	100 nM	No
5	Analyst, 2012, 137, 4913	Cavity based	100 nM	No
6	Chem. Commun., 2010, 46, 1070-1072	---	NR	Yes, (NR)

at 330 nm (the point of largest change in absorbance) shows linear increase ($R^2 = 0.9886$) in absorbance between 10^{-9} - 10^{-6} M ClO_4^- (Fig. 3B). The appearance of absorption tail from 320 to 650 nm indicates that on gradual addition of ClO_4^- , the relative amount of free molecules decreases and more aggregates are formed. The minimum detection limit for ClO_4^- was 1 nM.

The addition of other anions (100 μM) viz. F^- , Cl^- , Br^- , I^- , CN^- , OH^- , H_2PO_4^- , NO_3^- , AcO^- , HSO_4^- , SO_4^{2-} etc. caused insignificant change in the absorption spectrum of **CS-1** (Fig. S6, ESI[†]). The solution of **CS-1** (2 μM , HEPES buffer – 2% DMSO, pH 7.4) on excitation at λ_{ex} 290 nm exhibited emission maxima at 460 nm (quantum Yield, $\Phi = 0.35$)^{44,45}. On addition of aliquots of NaClO_4 , the fluorescence intensity at 460 nm was gradually quenched (Fig. 3C) and was associated with blue-shift of the emission maxima to 440 nm. The addition of all other anions (100 μM) viz. F^- , Cl^- , Br^- , I^- , CN^- , OH^- , H_2PO_4^- , NO_3^- , AcO^- , HSO_4^- , SO_4^{2-} or the addition of aromatics viz. benzene, toluene, phenol, benzoic acid, naphthalene and anthracene (50 μM each) etc. (Fig. S8, ESI[†]) caused an insignificant change in the fluorescence of **CS-1**. The insignificant change in the absorption intensity of **CS-1** at 290 nm i.e. at excitation wavelength clearly points that quenching of fluorescence intensity on addition of ClO_4^- ions to the solution of **CS-1** is not due to the decrease in the absorbance.

The plot of FI vs $[\text{ClO}_4^-]$ revealed that ~ 56% of the FI was quenched on addition of only 10 nM (0.005 equiv.) of ClO_4^- ions, thereby indicating a super-amplified quenching effect (Fig. 3D, inset). Therefore, when a ClO_4^- anion interacts with FOAs of **CS-1**, it may quench the emission of multiple fluorophores in its vicinity. The lowest detection limit⁴⁶ for the analysis of ClO_4^- was 10 pM. This is significantly lower than the permissible ClO_4^- concentration of 150 nM in drinking water.

The comparison of detection limits both in solution and solid state of **CS-1** with those of literature reports (Table 1) shows that **CS-1** is > 6000 times more sensitive than earlier reported probes for ClO_4^- . The Stern–Volmer plot for the quenching of fluorescence of FOAs of **CS-1** by ClO_4^- did not

follow linear equation $I_0/I = 1 + K_{\text{sv}}[Q]$. It gave non-linear Stern–Volmer curve which was well fitted to the exponential equation $(I/I_0 = A \exp(-K_{\text{sv}}[Q] + B))$ ^{28,29}, thereby confirming the super-amplified quenching at low concentrations of ClO_4^- . The K_{sv} values are found to be $2.42 \times 10^8 \text{ M}^{-1}$ and $3.59 \times 10^5 \text{ M}^{-1}$, respectively between 10^{-10} to 10^{-7} M and 10^{-7} to 10^{-5} M ClO_4^- concentration.

The semi-log plot of $\log [\text{ClO}_4^-]$ vs I_0/I shows linear increase between 10^{-10} - 10^{-7} M ($R^2 = 0.9929$) and 10^{-7} - 10^{-5} M ($R^2 = 0.9944$) ClO_4^- concentration. The minimum detection limit for ClO_4^- was 10 pM (Fig. 4). The titration of solution of **CS-1** with ClO_4^- in molecularly dissolved state i.e. in HEPES buffer – DMSO (80: 20) shows poor sensitivity towards ClO_4^- (LOD 2 μM) and highlights the role of aggregation of **CS-1** in enhanced sensitivity towards ClO_4^- in 98% HEPES buffer (Fig. S9, ESI[†]). The addition of 10 pM to 1000 nM ClO_4^- ions to the solution of **CS-1** (2 μM , HEPES buffer – 2% DMSO, pH 7.4) in steps with ten time increase in concentration shows change in fluorescence color of the solution from bluish green to blue (Fig. 4, inset). The analysis of Job's plot obtained by both absorbance and fluorescence as output channels shows the inflexion point near to 0.5 indicative of formation of 1:1 stoichiometric complex by **CS-1** with ClO_4^- (Fig. S10, ESI[†]).

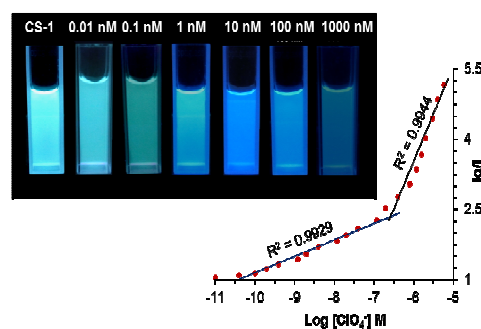


Fig 4. Plot of $\log [\text{ClO}_4^-]$ vs I_0/I showing change in I_0/I with increase in concentration of ClO_4^- from 10^{-11} to 10^{-5} M; inset shows visual changes in the emission intensity and color of the solution of **CS-1** (under illumination of 365 nm) in blank solution and upon addition of increasing concentration of ClO_4^- ions.

The selectivity of FOAs of **CS-1** towards ClO_4^- was further ascertained by the competition experiments where competing anions viz F^- , Cl^- , Br^- , I^- , CN^- , OH^- , H_2PO_4^- , NO_3^- , AcO^- , HSO_4^- , and SO_4^{2-} (100 μM each) were added to the solution of FOAs of **CS-1** before addition of ClO_4^- . As observed from the results, the fluorescence quenching efficiency of ClO_4^- remained by and large unaffected in the presence of several interfering anions (Fig. S11, ESI[†]). This indicates that **CS-1** is selective for recognition of ClO_4^- even in the presence of other anions. The FI of aggregates of **CS-1** remains constant between pH 4.7–8.7 and therefore permits the determination of ClO_4^- over this broad pH range (Fig. S12, ESI[†]).

The solution of molecular probe **CS-2** (2 μM , HEPES buffer 0.05 M – 2% DMSO, pH 7.4) did not undergo any change in its fluorescence intensity on addition of various anions viz F^- , Cl^- , Br^- , I^- , CN^- , OH^- , H_2PO_4^- , NO_3^- , AcO^- , HSO_4^- , SO_4^{2-} (100 μM) but the addition of ClO_4^- caused fluorescence quenching. On gradual addition of ClO_4^- ions to the solution of **CS-2**, the fluorescence intensity of **CS-2** remained unaltered even up to addition of 500 nM ClO_4^- and showed gradual decrease in fluorescence intensity only between 2–100 μM concentration of ClO_4^- ions. This is also associated with blue-shift of the emission maxima by 20 nm. The lowest limit of detection for ClO_4^- by **CS-2** is found to be 1.6 μM (Fig. 5). The analysis of Job's plot of **CS-2** and ClO_4^- obtained by fluorescence as output channel shows the inflexion point close to 0.5 equivalent and points to the formation of 1:1 complex (Fig. S13, ESI[†]). Therefore, probe **CS-2** though selectively binds with ClO_4^- but exhibits drastically decreased sensitivity in comparison to that observed for the probe **CS-1**.

Therefore, probe **CS-1** is nearly 10^5 times more sensitive towards ClO_4^- in comparison to probe **CS-2** and shows that the methyl substituents which though may not be directly interacting with ClO_4^- but drastically affect sensing properties of the **CS-1**.

Mechanism of interaction of **CS-1** with ClO_4^-

In order to provide an insight to the mechanism of interaction of FOAs of **CS-1** with ClO_4^- anion, the effect of concentration of ClO_4^- on the life time of **CS-1** was determined.

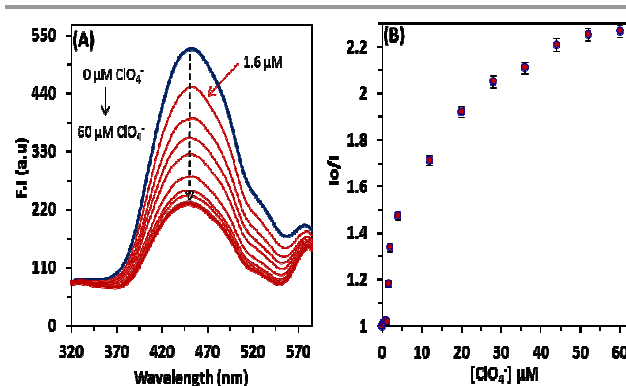


Fig 5. (A) Effect of gradual addition of ClO_4^- ions on the emission spectrum ($\lambda_{\text{ex}} = 290$ nm) of **CS-2** (2 μM , HEPES buffer – 2% DMSO, pH 7.4.); (B) Plot of I_0/I at 450 nm vs $[\text{ClO}_4^-]$ (Error bars show < 2.5% error).

The life time values were used to determine K_f (fluorescence decay constant) and K_{nr} (non-radiative decay constant) values at each concentration of ClO_4^- . The life time of **CS-1** remained constant at ~ 8.9 ns between ClO_4^- concentration 10^{-11} to 10^{-9} M but at higher concentrations of ClO_4^- , it gradually increased to 13.6 ns. The K_f values decreased gradually with the increase in concentration of ClO_4^- . The rate for non-radiative decay (K_{nr}) of the excited state of **CS-1** increased when concentration of ClO_4^- was raised from 10^{-11} to 10^{-9} M but at higher concentrations, K_{nr} also decreased gradually. In consonance with DLS and FE-SEM results, the FOAs of **CS-1** underwent further aggregation on addition of 10^{-11} to 10^{-9} M ClO_4^- . This ClO_4^- mediated further aggregation of free **CS-1** aggregates is associated with fluorescence quenching – a process commonly observed in literature⁴⁷. But at higher concentrations of ClO_4^- , the aggregates of **CS-1** underwent dissolution and the interactions of **CS-1** with ClO_4^- were gradually shifted to that at molecular level (Fig. 6). At molecular level, the cavity of **CS-1** formed by two 1-(biphenyl)benzimidazolium moieties undergoes coordination with ClO_4^- ion. It restricts the rotation of biphenyl rings and results in increased fluorescence life time from 8.9 to 13.6 ns. However, photo-induced electron transfer^{48,49} from biphenyl moiety to ClO_4^- ion results in formation of non-emissive excited state (Fig. S17) and results in efficient fluorescence quenching.

Therefore, probe **CS-1** follows static fluorescence quenching mechanism in the presence of 10^{-11} to 10^{-9} M ClO_4^- , but at higher concentrations i.e. at $> 10^{-9}$ M ClO_4^- concentration, the interaction of **CS-1** with ClO_4^- is shifted to dynamic process. ^1H NMR spectrum of **CS-1** and **CS-2** (DMSO- d_6 -H $_2$ O, 7:3) on addition of one equivalent of ClO_4^- show < 0.05 ppm up-field shift of Bim C2-H and ArH doublet and point to the weak interactions of **CS-1** and **CS-2** with ClO_4^- in molecularly dissolved state (Fig. S14–15, ESI[†]).

In order to evaluate the effect of methyl substituents on *m*-phenylene spacer on the conformations of the probes **CS-1** and **CS-2**, the U-conformational structures of the two molecules were optimized.

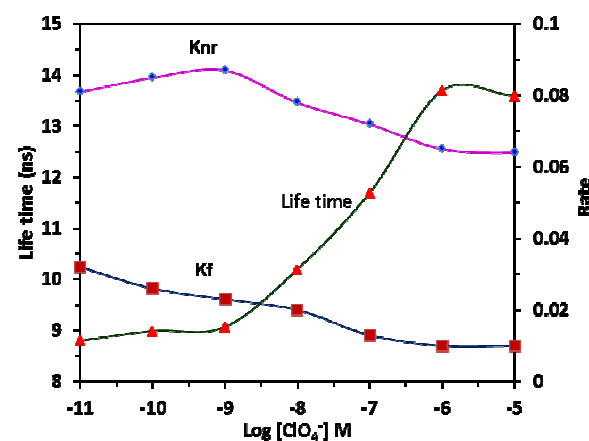


Fig 6. The life time, rate constants for radiative (k_f) and non-radiative (K_{nr}) decay of excited state of **CS-1** in the presence of different concentrations of ClO_4^- .

The super-imposition of energy minimized structures of **CS-1** and **CS-2** (Fig. 7A) shows that **CS-1** is optimized as a more compact structure with distance of 6.026 Å between C-2 carbons of benzimidazolium moieties. In case of **CS-2**, the distance between C-2 of two benzimidazolium moieties is increased to 6.713 Å. This difference in conformations of **CS-1** and **CS-2** could be assigned to the presence of three methyl substituents on *m*-phenylene ring which create enough steric bulk on CH₂ groups to decrease the cavity size of **CS-1**. Further, the energy minimized structures of 1:1 complexes of **CS-1** and **CS-2** reveal that **CS-1** has to undergo minimal change in its conformation during complex formation with ClO₄[−] anion. **CS-2** undergoes significant conformational change during complex formation with ClO₄[−]. The ClO₄[−] anion goes deep into the cavity of **CS-1** and three of its oxygen atoms form short contacts with BIM C2-H (2.13 – 2.38 Å) and ClO₄[−] oxygen atoms form anion-π interactions with π-cloud of the biphenyl and mesitylene rings. In **CS-2** - ClO₄[−] (1:1) complex, the π clouds of aryl rings do not participate in interaction with ClO₄[−]. Therefore, **CS-1** is better pre-organized to complex with ClO₄[−] than **CS-2** (Fig. S16-17, ESI[†]). Also, in addition to electrostatic interactions between ClO₄[−] and the benzimidazolium moieties of the **CS-1**, the efficiency of electron transfer from HOMO of **CS-1** to LUMO of ClO₄[−] may at least partly contribute to the selectivity of **CS-1** towards ClO₄[−]. The analysis of HOMO and LUMO of **CS-1** and its complex with ClO₄[−] shows that in case of free probe **CS-1**, the electron from biphenyl unit (HOMO) is excited to benzimidazolium ring (LUMO) but in its complex with ClO₄[−], the electron from biphenyl (HOMO) is transferred to ClO₄[−] (LUMO). This results in non-radiative excited state and is so responsible for fluorescence quenching in **CS-1**-ClO₄[−] complex.

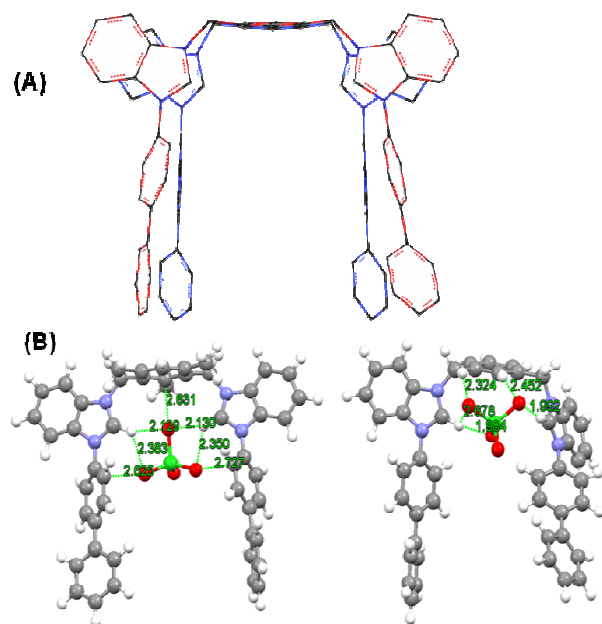


Fig 7. (A) The energy optimized structures of **CS-1** (blue) and **CS-2** (red) overlapped on each other; (B) The energy minimized structures of 1:1 complexes of **CS-1** and **CS-2** with ClO₄[−] (The structure were optimized using B3LYP with basis set 6-311G^{*}).

Thus combination of factors viz the aggregation of **CS-1** in water due to enhanced hydrophobicity and the better pre-organization of cavity in **CS-1** due to hydrophobicity and steric bulk of methyl substituents on linker between two benzimidazolium moieties in comparison to that in probe **CS-2** result in increased sensitivity and selectivity of **CS-1** towards ClO₄[−].

ClO₄[−] ions determination in tap water, soil samples and blood serum

In order to find the applications of **CS-1** for the determination of ClO₄[−] in tap water and in soil samples, a fixed amount of NaClO₄ was added to the tap water and soil samples. The soil samples were suspended in water. The water was filtered and was used for determination of ClO₄[−] using probe **CS-1**. Both categories of samples were analysed for 0.1 nM – 1000 nM concentrations of ClO₄[−] ions. The table 2 shows that in tap water samples maximum relative standard deviation was < 2.3% and pooled relative SD (PRSD) = 1.8%; the maximum relative error was < 1.6% and pooled relative error (PRE) was 1.3%. In case of soil samples maximum relative standard deviation was < 3.54% and pooled relative SD (PRSD) was 2.54%. The maximum relative error was < 2.9% and pooled relative error (PRE) was 1.96%. The results clearly show that **CS-1** can be used for determination of ClO₄[−] from both tap water and soil samples, though the errors and deviations are higher in case of soil samples than determined for tap water. Obviously, the soil contains more number of components than tap water, which leads to higher deviations.

Further to investigate the biological application, the fluorescence titration of **CS-1** (2 μM) was carried out in the presence of blood serum. It was found that in the presence of blood serum the maxima of **CS-1** was only marginally shifted from 460 nm to 450 nm. The presence of a new band at 330 nm could be attributed to the aromatic amino acids in the blood serum (Fig. S18, ESI[†]). On gradual addition of ClO₄[−] to the solution of **CS-1** containing blood serum, the gradual decrease in the fluorescence intensity was observed (Fig. 8).

Table 2 Application of **CS-1** in determination of ClO₄[−] in tap water and soil samples

Sr. No.	Conc. ClO ₄ [−] (nM)	Conc. determined ± SD ^a (μM)	Relative error (%)
Tap water			
1	0.1	0.11 ± 0.002	1.4
2	1	1.28 ± 0.021	1.5
3	10	10.5 ± 0.15	1.1
4	100	102.3 ± 2.1	1.6
5	1000	1001 ± 10.6	0.9
Soil samples			
1	0.1	0.12 ± 0.002	1.4
2	1	1.14 ± 0.04	2.9
3	10	10.3 ± 0.3	2.0
4	100	105.6 ± 3.6	2.4
5	1000	1011.7 ± 13.2	1.01

^aAverage ± standard deviation of three determinations

ARTICLE

Journal Name

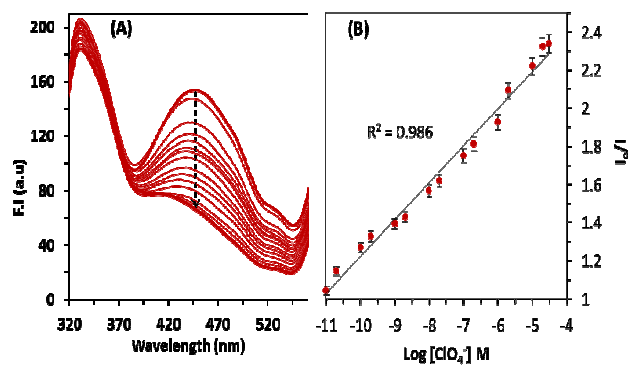


Fig 8. Effect of gradual addition of ClO₄⁻ ions on the emission spectrum ($\lambda_{\text{ex}} = 290$ nm) of CS-1 (2 μM) in blood serum and plot of $\log [\text{ClO}_4^-]$ vs I_0/I shows linear change with increase in concentration of ClO₄⁻ from 10^{-11} to 10^{-4} M (Error bars show < 3% error).

This decrease in intensity was also associated with blue-shift of the emission maxima by ~ 20 nm as observed in case of titration of CS-1 in HEPES buffer. The titration results showed

that ratio of I_0/I increases linearly with the increase in $\log [\text{ClO}_4^-]$ between 10 pM - 10 μM with $R^2 = 0.9860$. The lowest detection limit for the analysis of ClO₄⁻ was determined as 10 pM.

Contact mode detection of traces of ClO₄⁻

Finally we investigated the applicability of CS-1 in both qualitative and quantitative detection of ClO₄⁻ using contact mode method. For this we carried out experiments on paper strips coated with CS-1. The paper strips were then visualized under 365 nm UV light. We observed that the addition of 6 μL of 10^{-15} M ClO₄⁻ caused visible quenching of the fluorescence intensity on the paper strip [Fig. 9A(ii)] and colour of the drop casted area turned green, which is in consonance with solution phase studies. Complete quenching of fluorescence intensity was observed with 10^{-11} M ClO₄⁻ [Fig. 9A(vi)] and addition of higher concentrations of ClO₄⁻ results in dark colored area developed on paper strip. Fig. 9A(i) shows no quenching of fluorescence with water.

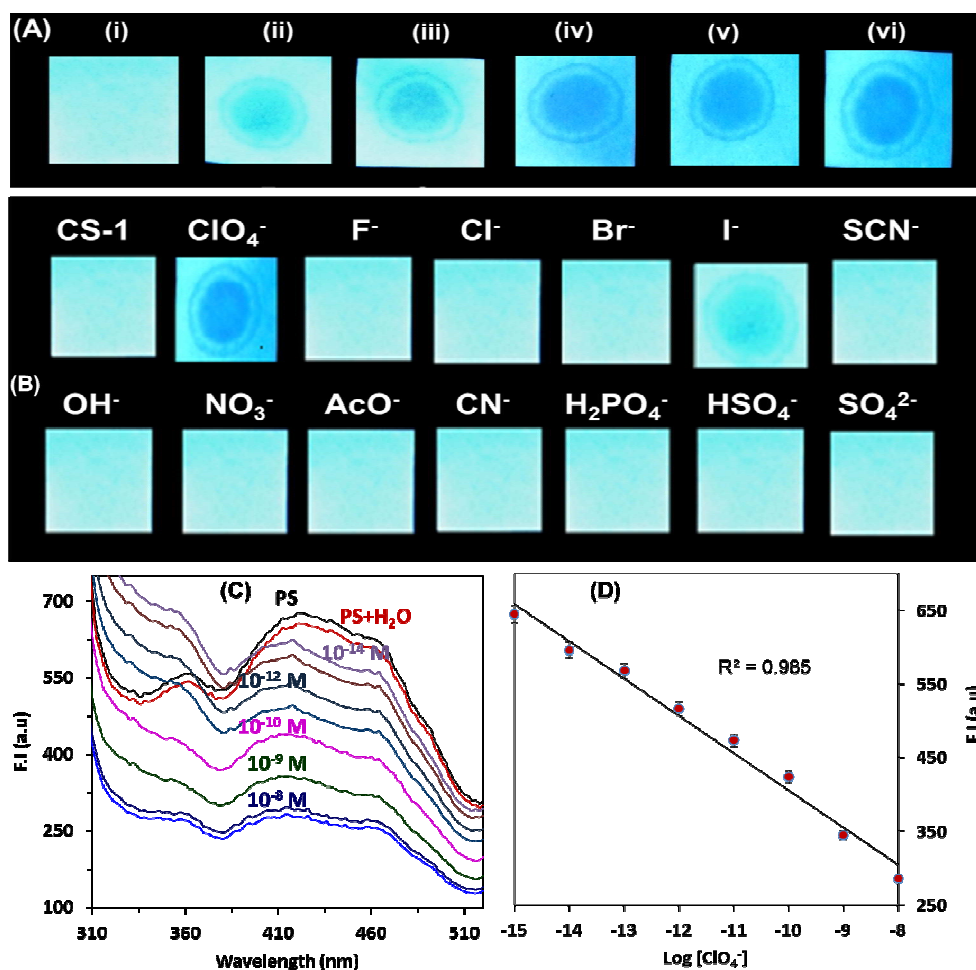


Fig 9. (A) Photographs of fluorescence quenching (under 365 nm UV light) of paper strips coated with CS-1 and different amounts of ClO₄⁻; (i) Paper strip with a drop of water; (ii) 10^{-15} M; (iii) 10^{-14} M; (iv) 10^{-13} M; (v) 10^{-12} M; (vi) 10^{-11} M ClO₄⁻ solution (6 μL). (B) Paper strips with addition of 10^{-11} M solutions (6 μL) of ClO₄⁻, F⁻, Cl⁻, Br⁻, I⁻, SCN⁻, OH⁻, NO₃⁻, AcO⁻, CN⁻, H₂PO₄⁻, HSO₄⁻ and SO₄²⁻ anions [The size of each paper strip is 1.0 cm²]. (C) Front surface steady-state fluorescence quenching of CS-1 with ClO₄⁻. PS = fluorescence spectrum of CS-1 coated paper strip; PS + water = spectrum after addition of 200 μL of water to PS. 10^{-14} to 10^{-8} corresponds to molar concentrations of ClO₄⁻ added to PS; (D) Plot of fluorescence intensity of CS-1 vs $\log [\text{ClO}_4^-]$ (M) (error < 2.8%).

Journal Name

ARTICLE

Therefore, the minimum amount of ClO_4^- detectable is $6 \times 10^{-19} \text{ g/cm}^2$ under 365 nm light illumination. For $6 \mu\text{L}$ of 10^{-15} M solution, amounts to ~ 3600 molecules of ClO_4^- . Further to analyse the selectivity of **CS-1** towards ClO_4^- in comparison to other anions, 10^{-11} M solution ($6 \mu\text{L}$) of each of the following anions F^- , Cl^- , Br^- , I^- , CN^- , OH^- , H_2PO_4^- , NO_3^- , AcO^- , HSO_4^- , and SO_4^{2-} was added on the **CS-1** coated paper strip and change in their fluorescence was observed. The results clearly reveal (Fig. 9B) that even on addition of 10000 times higher amounts of each of these anions than LOD of ClO_4^- (10^{-15} M), only a small change in fluorescence was observed only with iodide ions, which is well known to be the most interfering species with ClO_4^- due to similar size and basicity. The other anions did not cause any observable change in fluorescence of **CS-1** coated paper strip. Therefore, **CS-1** coated paper strips are 10000 times or more selective towards ClO_4^- over the other anions studied.

In order for quantification of ClO_4^- using **CS-1** coated paper strips, the fluorescence spectra of the above paper strips treated with different concentrations of ClO_4^- were recorded. The fluorescence spectrum of the paper strip coated with **CS-1** exhibits broad spectrum between 370 – 500 nm with two maxima at 430 and 470 nm which is in contrast to a sharp maxima at 460 nm in aggregate state of **CS-1** in solution phase. Therefore, in solid state, the aggregation behaviour of **CS-1** is different from that in the solution phase. The intensity of the fluorescence spectrum gradually decreases with the gradual increase in concentration of solution of ClO_4^- (Fig. 9C). The plot of fluorescence intensity vs $\log [\text{ClO}_4^-]$ shows linear change and is in agreement with exponential decrease in fluorescence intensity (Fig. 9D) with addition of ClO_4^- as observed in the solution phase. The Ksv value as determined by exponential equation $I/I_0 = A e^{K_{sv}[Q]} + B$ is found to be $1.49 \times 10^8 \text{ M}$ and is in close agreement with K_{sv} ($2.42 \times 10^8 \text{ M}^{-1}$) that observed in solution phase for the $[\text{ClO}_4^-]$ below 10^{-9} M . The addition of water ($200 \mu\text{L}$) caused only a small quenching of fluorescence intensity of the paper strip. Therefore, paper strips coated with **CS-1** were highly sensitive towards ClO_4^- and could be used for quantification of 10^{-14} M – 10^{-8} M ClO_4^- solutions.

3. Experimental Section

General details of instruments, sample preparation are given in supporting information.

Synthesis of CS-1

The solution of 1-(4-biphenyl)benzimidazole (**1**) (270 mg, 1 mmol) and 2,4-bis(bromomethyl)-1,3,5-trimethylbenzene (**2**)

(153 mg, 0.5 mmol) was heated in DMF (3 ml) at 100°C under N_2 atm for 24 h. After completion of the reaction, the solvent was removed under vacuum. The crude residue was dissolved in methanol and was filtered to remove suspended impurities. To this filtrate, aqueous solution of NH_4PF_6 (163 mg, 1 mmol) was added drop wise with continuous stirring and stirring was continued for 7–8 h. The white solid separated was filtered to get **CS-1** as white solid (460 mg); yield 94 %; m.p. 247°C ; ^1H NMR (500MHz, $\text{DMSO}-d_6$): δ 2.34 (s, 3H, CH_3), 2.47 (s, 6H, 2 x CH_3), 5.84 (s, 4H, 2 x CH_2), 7.34 (s, 1H, ArH), 7.38 – 7.44 (m, 6H, ArH), 7.58 (d, 4H, $J = 7.5 \text{ Hz}$), 7.79 – 7.90 (m, 14H, ArH), 8.38 (d, 2H, $J = 8.5 \text{ Hz}$, ArH), 9.46 (s, 2H, BimC2H); ^{13}C (125 MHz, $\text{DMSO}-d_6$): δ 15.9, 20.1, 46.2, 127.0, 127.2, 127.3, 127.5, 128.3, 128.4, 128.8, 129.7, 132.0, 132.6, 132.7, 138.7, 140.6, 141.3, 141.4, 142.5; HRMS m/z (TOF MS ES+) calculated for $\text{C}_{49}\text{H}_{42}\text{F}_{12}\text{N}_4\text{P}_2$ [**CS-1** – PF_6] 831.3046, found 831.3148 [**CS-1** – PF_6] (40%), m/z calculated for [**CS-1** – 2PF_6] $^{2+}$ 343.1699, found 343.1758 [**CS-1** – 2PF_6] $^{2+}$ (100%).

Synthesis of CS-2

The reaction of 1-(4-biphenyl)benzimidazole (**1**) (270 mg, 1 mmol) and 1,3-bis(bromomethyl)benzene (**3**) (132 mg, 0.5 mmol) as described above gave chemosensor **CS-2**, white solid (460 mg); yield 95.3 %; m.p. 232°C ; ^1H NMR (500 MHz, $\text{DMSO}-d_6$): δ 5.89 (s, 4H, 2 x CH_2), 7.48 (d, 2H, $J = 7.0 \text{ Hz}$, ArH), 7.54 (t, 5H, $J = 7.5 \text{ Hz}$, ArH), 7.66 – 7.74 (m, 6H, ArH), 7.79 (d, 4H, $J = 7.5 \text{ Hz}$, ArH), 7.85 (s, 1H, ArH), 7.93 (t, 6H, $J = 9.0 \text{ Hz}$, ArH), 7.98 (d, 2H, $J = 8.5 \text{ Hz}$, ArH), 8.05 (d, 4H, $J = 8.5 \text{ Hz}$, ArH), 10.33 (s, 2H, BimC2H); ^{13}C (125 MHz, $\text{DMSO}-d_6$): δ 50.6, 114.3, 114.6, 126.2, 127.4, 127.6, 128.1, 128.9, 129.5, 129.7, 130.2, 131.3, 131.7, 132.7, 134.8, 138.9, 142.7, 143.3; HRMS m/z (TOF MS ES+) calculated for $\text{C}_{46}\text{H}_{36}\text{F}_{12}\text{N}_4\text{P}_2$ [**CS-2** – PF_6] $^+$ 789.2576, found 789.2882 [**CS-2** – PF_6] $^+$ (40%), m/z calculated for [**2** – PF_6] $^{2+}$ 322.1465, found 322.1618 [**CS-2** – 2PF_6] $^{2+}$ (100%).

Conclusions

Thus, probe **CS-1** undergoes self-assembly to form fluorescent organic aggregates (FOAs) which further undergo aggregation in the presence of 10^{-11} – 10^{-9} M ClO_4^- and dis-aggregation with ClO_4^- at concentration $> 10^{-9} \text{ M}$, as revealed by both DLS and FE-SEM studies. This is associated with super-amplified fluorescence quenching in the presence of ClO_4^- ions following two domains of non-linear complexation with K_{sv} values $2.42 \times 10^8 \text{ M}^{-1}$ and $3.59 \times 10^5 \text{ M}^{-1}$. The lowest limit of detection of ClO_4^- is 10 pM in solution phase and $6 \times 10^{-18} \text{ g/cm}^2$ by contact mode method and quantitatively measuring front surface steady state fluorescence using paper strips coated with **CS-1**. FOAs of

ARTICLE

Journal Name

CS-1 find applications in determination of ClO_4^- from tap water, soil and also in the presence of blood serum. The life-time measurement studies, K_f and K_{nr} results highlight the participation of both dynamic and static mechanisms depending on the concentration of ClO_4^- . Therefore, the present study provides a new insight into the design of self-assembled molecular probes for the detection of ClO_4^- ions.

Acknowledgements

This work was supported by Department of Science and Technology, New Delhi (SR/S1/OC-75/2012). We thank UGC for UPE programme to the university and CAS status to the department and DST for FIST programme. RK and SS acknowledge UGC and DST for fellowships.

Notes and references

- 1 P. A. Gale, N. Busschaert, C. J. E. Haynes, L. E. Karagiannidis, I. L. Kirby, *Chem. Soc. Rev.*, 2014, **43**, 205–241.
- 2 L. E. S. Figueroa, M. E. Moragues, E. Climent, A. Agostini, R. Martinez-Manez, F. Sancenon, *Chem. Soc. Rev.*, 2013, **42**, 3489–3613.
- 3 X. Li, X. Gao, W. Shi, H. Ma, *Chem. Rev.* 2013, **114**, 590–659.
- 4 H. J. Kim, M. H. Lee, L. Mutihac, J. Vicens, J. S. Kim, *Chem. Soc. Rev.*, 2012, **41**, 1173–1190.
- 5 Y. Zhou, J. Yoon, *Chem Soc. Rev.* 2012, **41**, 52–67.
- 6 M. Wenzel, J. R. Hiscock, P. A. Gale, *Chem. Soc. Rev.*, 2012, **41**, 480–520.
- 7 N. Kaur, S. Kumar, *Tetrahedron*, 2011, **67**, 9233–9264.
- 8 Y. Zhou, Z. Xu, J. Yoon, *Chem. Soc. Rev.*, 2011, **40**, 2222–2235.
- 9 P. A. Gale, *Chem. Soc. Rev.*, 2010, **39**, 3746–3771.
- 10 C. Caltagirone, P. A. Gale, *Chem. Soc. Rev.*, 2009, **38**, 520–563.
- 11 X. Chen, X. Tian, I. Shin, J. Yoon, *Chem. Soc. Rev.*, 2011, **40**, 4783–4804.
- 12 J. Ma, P. K. Dasgupta, *Anal. Chim. Acta.*, 2010, **673**, 117–125.
- 13 D. T. Quang, J. S. Kim, *Chem. Rev.*, 2010, **110**, 6280–6301.
- 14 K. Kaur, R. Saini, A. Kumar, V. Luxami, N. Kaur, P. Singh, S. Kumar, *Coord. Chem. Rev.*, 2012, **256**, 1992–2028.
- 15 H. S. Jung, X. Chen, J. S. Kim, J. Yoon, *Chem. Soc. Rev.*, 2013, **42**, 6019–6031.
- 16 Y. Yang, Q. Zhao, W. Feng, F. Li, *Chem. Rev.*, 2013, **113**, 192–270.
- 17 F. Wang, L. Wang, X. Chen, J. Yoon, *Chem. Soc. Rev.*, 2014, **43**, 4312–4324.
- 18 J. Suk, Z. Wu, L. Wang and A. J. Bard, *J. Am. Chem. Soc.*, 2011, **133**, 14675–14685.
- 19 Q. Zhao, K. Li, S. Chen, A. Qin, D. Ding, S. Zhang, Y. Liu, B. Liu, J. Z. Sun and B. Z. Tang, *J. Mater. Chem.*, 2012, **22**, 15128–15135.
- 20 J. Wang, X. Xu, L. Shi, and L. Li, *ACS Appl. Mater. Interfaces.*, 2013, **5**, 3392–3400.
- 21 H. Sharma, A. Singh, N. Kaur, and N. Singh, *ACS Sustainable Chem. Eng.*, 2013, **1**, 1600–1608.
- 22 X. Zhang, X. Zhang, B. Yang, Y. Zhang, and Y. Wei, *ACS Appl. Mater. Interfaces.*, 2014, **6**, 3600–3606.
- 23 A. Singh, S. Kaur, A. Kaur, T. Aree, N. Kaur, N. Singh and M. S. Bakshi, *ACS Sustainable Chem. Eng.*, 2014, **2**, 982–990.
- 24 H. Sharma, V. K. Bhardwaj, and N. Singh, *Eur. J. Inorg. Chem.*, 2014, 5424–5431.
- 25 A. Singh, T. Raj, T. Aree and N. Singh, *Inorg. Chem.*, 2013, **52**, 13830–13832.
- 26 S. Sandhu, R. Kumar, P. Singh, A. Mahajan, M. Kaur and S. Kumar, *ACS Appl. Mater. Interfaces.*, 2015, **7**, 10491–10500.
- 27 S. Kumar, P. Singh, A. Mahajan and S. Kumar, *Org. Lett.*, 2013, **15**, 3400–3403.
- 28 H. Feng, Y. Zheng, *Chem. Eur. J.*, 2014, **20**, 195–201.
- 29 L. Zhang, C. Zhao, J. Zhou and T. Kondo, *J. Mater. Chem. C.*, 2013, **1**, 5756–5764.
- 30 V. Balzani, P. Ceroni, S. Gestermann, C. Kauffmann, M. Gorka and F. Vogtle, *Chem. Commun.*, 2000, 853–854.
- 31 Y. Sun, Z. Chen, E. Puodziukynaite, D. M. Jenkins, J. R. Reynolds and K. S. Schanze, *Macromolecules*, 2012, **45**, 2632–2642.
- 32 B. C. Blount, D. Q. Rich, L. Valentin-Blasini, S. Lashley, C. V. Ananth, E. Murphy, J. C. Smulian, B. J. Spain, D. B. Barr, T. Ledoux, P. Hore and M. Robson, *Environ. Sci. Technol.*, 2009, **43**, 7543–7549.
- 33 T. Zhang, Q. Wu, H. W. Sun, J. Rao, K. Kannan, *Environ. Sci. Technol.*, 2010, **44**, 6947–6953.
- 34 M. A. Saeed, J. J. Thompson, F. R. Fronczek and Md. A. Hossain, *Cryst. Eng. Commun.*, 2010, **12**, 674–676.
- 35 L. Yang, Y. Li, L. Jiang, X. Feng and T. B. Lu, *Cryst. Eng. Commun.*, 2009, **11**, 2375–2380.
- 36 M. J. Hynes, B. Maubert, V. McKee, R. M. Town and J. Nelson, *J. Chem. Soc. Dalton Trans.*, 2000, 2853–2859.
- 37 G. Morgan, V. McKee and J. Nelson, *Chem. Commun.*, 1995, 1649–1652.
- 38 S. D. Taylor, W. Howard, N. Kaval, R. Hart, J. A. Krause and W. B. Connick, *Chem. Commun.*, 2010, **46**, 1070–1072.
- 39 R. Kumar, S. Kumar, P. Singh, G. Hundal, M. S. Hundal and S. Kumar, *Analyst.*, 2012, **137**, 4913–4916.
- 40 P. Singh, L. S. Mittal, V. Vanita, R. Kumar, G. Bhargava, A. Walia and S. Kumar, *Chem. Commun.*, 2014, **50**, 13994–13997.
- 41 A. Sahana, A. Banerjee, S. Lohar, A. Chottapadhyay, S. K. Mukhopadhyay and D. Das, *RSC Adv.*, 2013, **3**, 14044–14047.
- 42 C. Gao, G. Gao, J. Lan and J. You, *Chem. Commun.*, 2014, **50**, 5623–5625.
- 43 K. Kaur, V.K. Bhardwaj, N. Kaur and N. Singh, *Inorg. Chem. Commun.*, 2012, **26**, 31–36.
- 44 W. H. Melhuish, *J. Phys. Chem.*, 1961, **65**, 229–235.
- 45 J. N. Demas, G. A. Crosby, *J. Phys. Chem.*, 1971, **75**, 991–1024.
- 46 J. Mokac, A. M. Bond, S. Mitchell, G. Scollary, *Pure Appl. Chem.*, 1997, **69**, 297–328.
- 47 Z. Zhelev, H. Ohba, R. Bakalova, *J. Am. Chem. Soc.*, 2006, **128**, 6324–6325.
- 48 A. Li, J. Wang, F. Wang, Y. Jiang, *Chem. Soc. Rev.*, 2010, **39**, 3729–3745.
- 49 T. Gunnlaugsson, H. D. P. Ali, M. Glynn, P. E. Kruger, G. M. Hussey, F. M. Pfeffer, C. M. G. Santos, J. Tierney, *Journal of Fluorescence*, 2005, **15**, 287–299.